Accurate Shadow Region Imaging Algorithm Using Ellipse Extrapolation Based on Distorted Hyperbola Fitting for UWB Radars

Yoriaki Abe, *Shouhei Kidera*, and *Tetsuo Kirimoto*
Graduate School of Informatics and Engineering, The University of Electro-Communications, 1-5-1, Chofugaoka, Chofu, Tokyo, 182-8585, Japan.
E-mail: abe@secure.ee.uec.ac.jp

Abstract

Ultra-wideband (UWB) pulse radars have a definitive advantage in high-range resolution imaging and are suitable for near-field measurements, particular in the case of a rescue robot or security sensor, where an optical sensor is unsuitable. Although we have already proposed an accurate imaging algorithm called Range Points Migration (RPM), the reconstructible area of RPM is too small to identify an object shape when the object is far from the observation site in the case of limited aperture size. To resolve the problem, this paper proposes a novel image expansion method based on ellipse extrapolation, which is converted to distorted hyperbola fitting in the data space to enhance extrapolation accuracy. Numerical simulations show that the proposed method accurately extrapolates the target boundary, even if an extremely small region of the target boundary is obtained by the RPM.

1 Introduction

UWB pulse radars have great potential for near-field measurement with high range resolution, even in critical situations such as disaster or resource exploration scenes, where an optical measurement is barely applicable owing to dust in the air or a high concentration of certain gases. In recent years, various radar imaging algorithms based on data synthesis, such as the synthetic aperture radar (SAR) algorithm [1], time-reversal algorithms [2], and range migration methods [3], have been proposed. However, their computational costs are often impractically large for real-time applications such as robotic or security sensors. On the other hand, we have proposed the accurate imaging algorithm RPM, which directly converts a group of range points to a group of target points through accurate estimation of the direction of arrival [4]. However, when an object is far from the observation site owing to the presence of obstacles such as rubble in a disaster area, the reconstruction area of the RPM is too narrow to recognize objects as human bodies or other objects, and this is an inherent and common problem in all conventional approaches. To capture the size or rough shape of a target, this paper proposes an accurate target boundary extrapolation method based on ellipse fitting. While the estimated target points are used to fit an ellipse in a scheme typically employed for this task, the approach is extremely sensitive to imaging error, especially if only a small region of the ellipse can be obtained. To overcome this difficulty, the proposed method converts conventional ellipse fitting to distorted hyperbola fitting using range points, which are directly extracted from the observation data. Numerical simulations show that even if an extremely small region on the target boundary is reconstructed by RPM, the proposed method accurately extrapolates the target boundary avoiding the effect of errors in RPM mapping.

2 System Model

Figure 1 shows the system model. The model assumes that targets have arbitrary shapes with clear boundaries. It employs a mono-static radar system, where an omni-directional antenna scans along an arbitrary curve. We also assume that the propagation speed of the radio wave is known and constant. We use a mono-cycle pulse as the transmitting current. The space in which the targets and antenna are located is expressed by the parameters (x, z). The parameters are normalized by λ, which is the central wavelength of the pulse. $s'(X, Z, t)$ is defined as the electric field received at the antenna location $(x, z) = (X, Z)$ at time t. $s(X, Z, t)$ is the output of the Wiener filter multiplied by the envelope of the output of the matched filter and it maintains the accuracy and resolution. The definition and filtering procedure of the Wiener filter are given in [4]. $s(X, Z, t)$ is converted to $s(X, Z, R')$ with $R' = \mathrm{c}_0 t/2\lambda$, where c_0 is the speed of the radio wave. The group of (X, Z, R) so-called range points are extracted from the local peaks of $s(X, Z, R')$ as,

$$\frac{\partial s(X, Z, R')}{\partial R'} = 0,$$
$$s(X, Z, R') \geq \alpha \max s(X, Z, R'). \tag{1}$$

The parameter $\alpha > 0$ is empirically determined.

3 Conventional Method

This section describes a typical scheme for fitting an ellipse using the target boundary points. As a practical assumption, the target boundary is approximated as a set of ellipses because the human body is generally assumed to be composed of a set of ellipsoids. Figure 2 shows the scheme of the conventional method. First, target points produced by the RPM are obtained from the extracted range points. To classify the obtained target points into multiple ellipse objects, each target point is clustered according to Euclidean distance, which is detailed in Section 4. Here, we define $\boldsymbol{P} = (a, b, X_c, Z_c, \theta)$ as parameters of the ellipse whose major axis is a, minor axis is b, center of focal points is (X_c, Z_c), and angle from the x axis to the major axis is θ. This method applies ellipse fitting to the target points in each cluster. $\boldsymbol{P}_i$ for the ith cluster's ellipse is determined as

$$\boldsymbol{P}_i = \arg\min_{\boldsymbol{P}} \sum_{k=1}^{N_i} \parallel \boldsymbol{r}_{k,i} - \boldsymbol{r}_k(\boldsymbol{P}) \parallel^2, (i = 1, ..., C), \tag{2}$$

where $\boldsymbol{r}_{k,i} = (x_{k,i}, z_{k,i})$ denotes the location of the kth target point in the ith cluster and $\boldsymbol{r}_k(\boldsymbol{P})$ denotes the location of the foot of a perpendicular from (X_k, Z_k) to the ellipse expressed by $\boldsymbol{P}$. N_i denotes the total number of target points in the ith cluster, and C denotes the total number of clusters. It is predicted that this method ensures accuracy in ellipse fitting if a sufficient area of an ellipse is reconstructed by the RPM. However, if the target points are distributed in a small region of the target boundary, the accuracy of this method severely deteriorates because it is extremely susceptible to errors in RPM mapping.

4 Proposed Method

To avoid the problem mentioned above, we propose a novel image expansion method based on the distorted hyperbola fitting of observed range points. In principle, an ellipse curve in the target space is converted to a distorted hyperbolic curve in the range space. Thus, to be impervious to errors in RPM mapping, the proposed method employs range points for ellipse extrapolation. Figure 3 shows the scheme of the proposed method, where ϕ denotes the antenna location as shown in Figure 2. In this method, $\boldsymbol{P}_i$ for the ith cluster is determined as

$$\boldsymbol{P}_i = \arg\min_{\boldsymbol{P}} \sum_{k=1}^{N_i} \left| \{R_{k,i} - R_k(\boldsymbol{P})\} \left(\frac{d_{k,i}^2}{\beta} + 1 \right) \right|^2, (i = 1, ..., C), \tag{3}$$

where $R_{k,i}$ denotes the range point corresponding to the kth target point in the ith cluster and $R_k(\boldsymbol{P})$ denotes the orthogonal distance from (X_k, Z_k) to the ellipse expressed by $\boldsymbol{P}$. Here, up to four boundary points on the ellipse can satisfy the previous orthogonal condition. We then choose the one boundary point that has the minimum distance to the target points $\boldsymbol{r}_{k,i}$ created by RPM. $d_{k,i}$ is the minimum distance from $(X_{c,i}, Z_{c,i})$ to the line connecting the points (X_k, Z_k) and $\boldsymbol{r}_{k,i}$, as shown in Figure 1. The constant β is empirically determined. The weight function $(d_{k,i}^2/\beta + 1)$ in (3) prevents the deviation of the center of the focus of the ellipse from the actual center. The procedure of the proposed method is summarized as follows.

Step 1). A set of target points $\mathcal{T}_{\rm rpm}$ is obtained by applying RPM to observed range points.

Step 2). The two nearest target points in $\mathcal{T}_{\rm rpm}$ are recursively combined as one cluster, until the distance for all pairs of clusters is $D_{i,j} \leq \gamma$, where the constant γ is empirically determined. Here, $D_{i,j}$ is defined as

$$D_{i,j} = \frac{1}{n_i n_j} \sum_{k=1}^{n_i} \sum_{l=1}^{n_j} \parallel \boldsymbol{r}_{k,i} - \boldsymbol{r}_{l,j} \parallel, \tag{4}$$

where n_i and n_j denote the numbers of target points in clusters C_i and C_j, respectively. $\boldsymbol{r}_{k,i}$ and $\boldsymbol{r}_{l,j}$ are the positions of target points. All points in $\mathcal{T}_{\rm rpm}$ are then classified into multiple clusters.

Step 3). For each cluster, the parameter $\boldsymbol{P}$ is determined with Eq. (3). Here, $R_k(\boldsymbol{P})$ is determined by

$$R_k(\boldsymbol{P}) = \min_n \parallel \boldsymbol{r}_{k,i} - \boldsymbol{r}_k^n(\boldsymbol{P}) \parallel, \tag{5}$$

where $\boldsymbol{r}_k^n(\boldsymbol{P})$ denotes the boundary points of the ellipse, whose tangent is perpendicular to the line from (X_k, Z_k) to $\boldsymbol{r}_{k,i}$, and n is as high as four as previously described.

While the target points obtained by RPM are employed for clustering or distance measurement for an ellipse in Step 2), the fitting process itself, is completed without RPM mapping. Therefore, the fitting accuracy of this method depends on only the range errors and is much higher than that of the conventional approach.

5 Numerical Simulations

This section investigates the performance of each method. Six ellipse targets are assumed in this case. An omni-directional antenna scans along a circle whose center is $(x, z) = (2.5, 0)$ and radius is 2.5λ. Figure 4 shows the range points (X, Z, R), where ϕ denotes the angle as shown in Figure 1. The true range points are given in this case. Figure 5 shows the image estimated using the conventional method described in Section 3. Here, the simulated annealing algorithm is employed to obtain a global optimum, where the Levenberg Marquardt method is sequentially involved for local optimization. This example shows that even though the observed ranges have no errors, the accuracy of the conventional method deteriorates owing to the estimation errors of RPM mapping. On the other hand, Figure 6 shows the image estimated using the proposed method. $\alpha = 0.3, \beta = 60$, and $\gamma = 3\lambda$ are set. This result shows that the proposed method accurately fits ellipses to all targets, even if an extremely small region of the target boundary is theoretically reconstructed in many cases. Figure 7 shows the image estimated using the proposed method in a noisy environment. The received signal $s'(X, Z, R)$ is based on the geometrical optics approximation with propagation attenuation. Gaussian white noise is added to the received signals, and the S/N is 30 dB in this case, which is practical for a real UWB radar system [5]. Here, the S/N is defined as the ratio of peak instantaneous signal power to the averaged noise power after applying the matched filter. The figure shows that in a noisy situation, the accuracy of the proposed method deteriorates owing to errors in the observed ranges. However, it is verified that Eq. (3) in the proposed method suppresses the deviation of the estimated parameters of an ellipse from actual parameters.

As a reference example, the SAR method extended to the near field [4] is investigated. Figure 8 shows an example of SAR in a noiseless environment for the same targets as in Figure 5. It is obvious from the result that this method creates many unnecessary images far from the actual boundary, and it is hence difficult to apply the target boundary extrapolation method based on ellipse fitting to SAR.

6 Conclusion

This paper first introduced the target-boundary extrapolation scheme as a conventional method that employs ellipse fitting with target points obtained by the RPM. We then presented an example of this method, showing that even small errors of the target points critically distort the extrapolation. Secondly, we proposed a novel extrapolation method, which uses observed range points to fit the distorted hyperbolic curve. Numerical simulations show that the proposed method accurately extrapolates multiple ellipse target boundaries, even if an extremely small region is obtained. In future work, we will enhance the accuracy in a noisy environment.

7 References

1. D. L. Mensa, G. Heidbreder and G. Wade, "Aperture Synthesis by Object Rotation in Coherent Imaging," *IEEE Trans. Nuclear Science.,* vol. 27, no. 2, pp. 989–998, Apr., 1980.

2. A. Marengo, F. K. Gruber, and F. Simonetti, "Time-Reversal MUSIC Imaging of Extended Targets," *IEEE Trans. Image Process.,* vol. 16, no. 8, pp. 1967–1984, Aug. 2007.

3. F. Soldovieri, A. Brancaccio, G. Prisco, G. Leone, and R. Pieri, "A Kirchhoff-based shape reconstruction algorithm for the multimonostatic configuration: The realistic case of buried pipes," *IEEE Trans. Geosci. Remote Sens.,* vol. 46, no. 10, pp. 3031–3038, Oct. 2008.

4. S. Kidera, T. Sakamoto, T. Sato, "Accurate UWB Radar 3-D Imaging Algorithm for Complex Boundary without Range Points Connections," *IEEE Trans. Geosci. Remote Sens.,* vol.48, no. 4, pp. 1993–2004, Apr., 2010.

5. S. Kidera, T. Sakamoto, T. Sato, "Super-Resolution UWB Radar Imaging Algorithm Based on Extended Capon with Reference Signal Optimization," *IEEE Trans. Antennas and Propagation,* Apr., 2011. (in press)

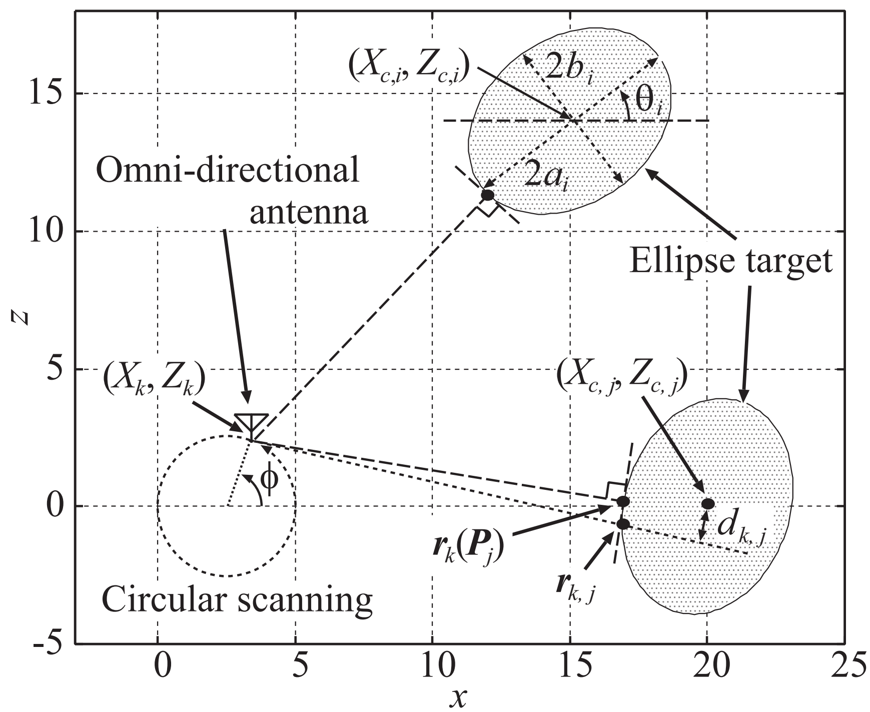

Figure 1: System model.

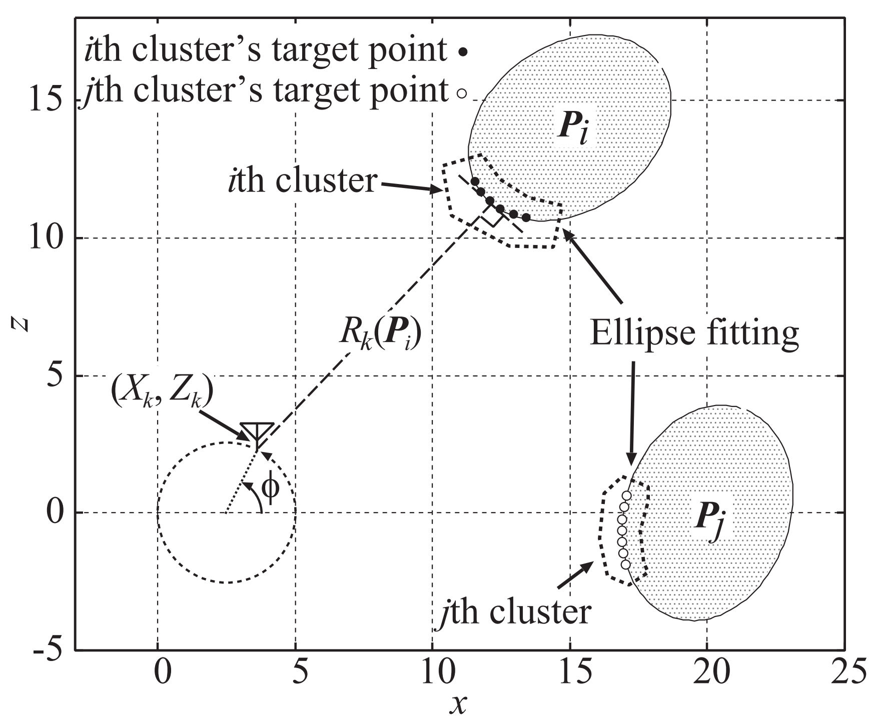

Figure 2: Conventional scheme for ellipse extrapolation.

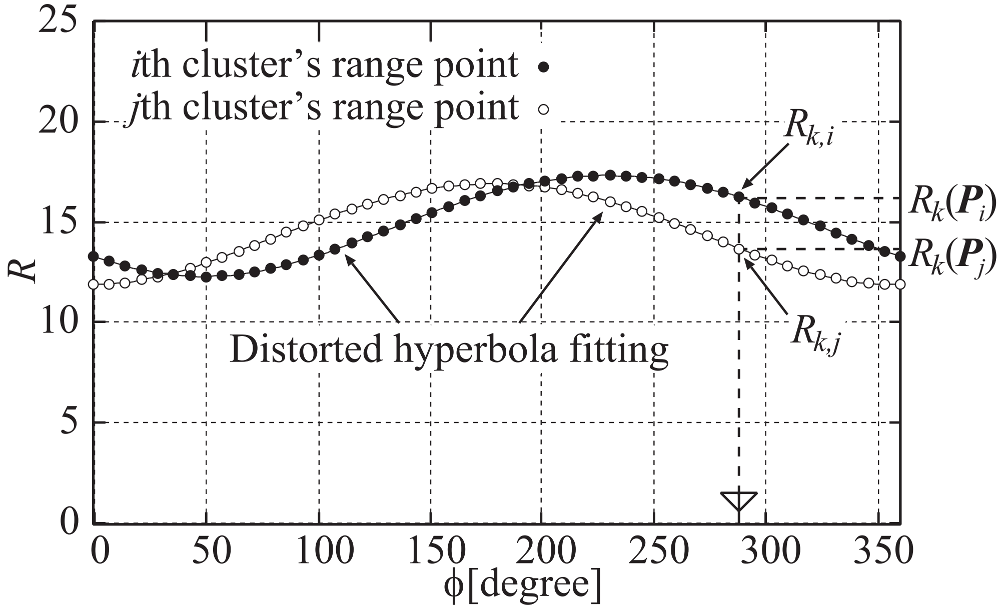

Figure 3: Proposed scheme for ellipse extrapolation.

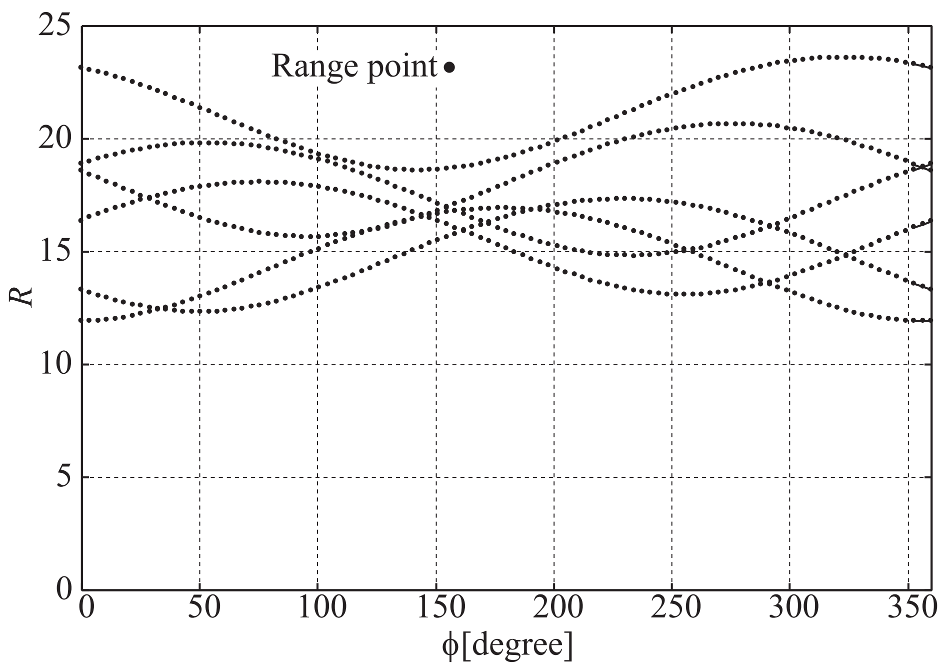

Figure 4: Extracted range points for six ellipses in noiseless situation.

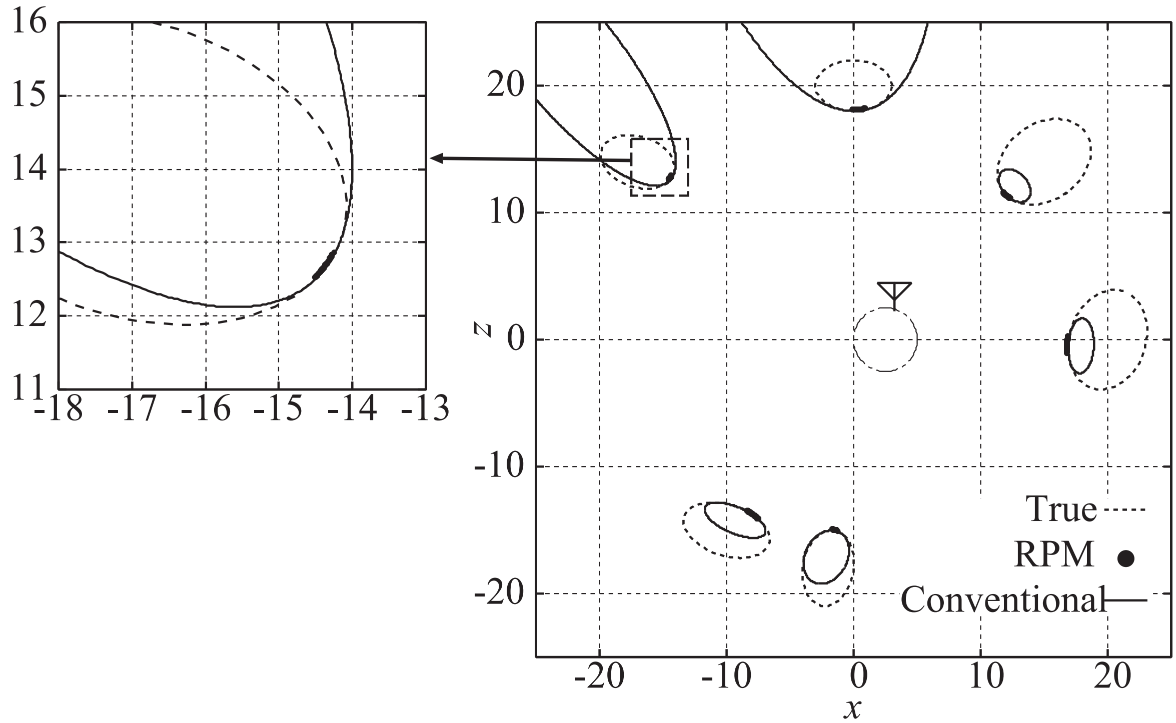

Figure 5: Target points obtained by the RPM and their extrapolation image by the conventional method.

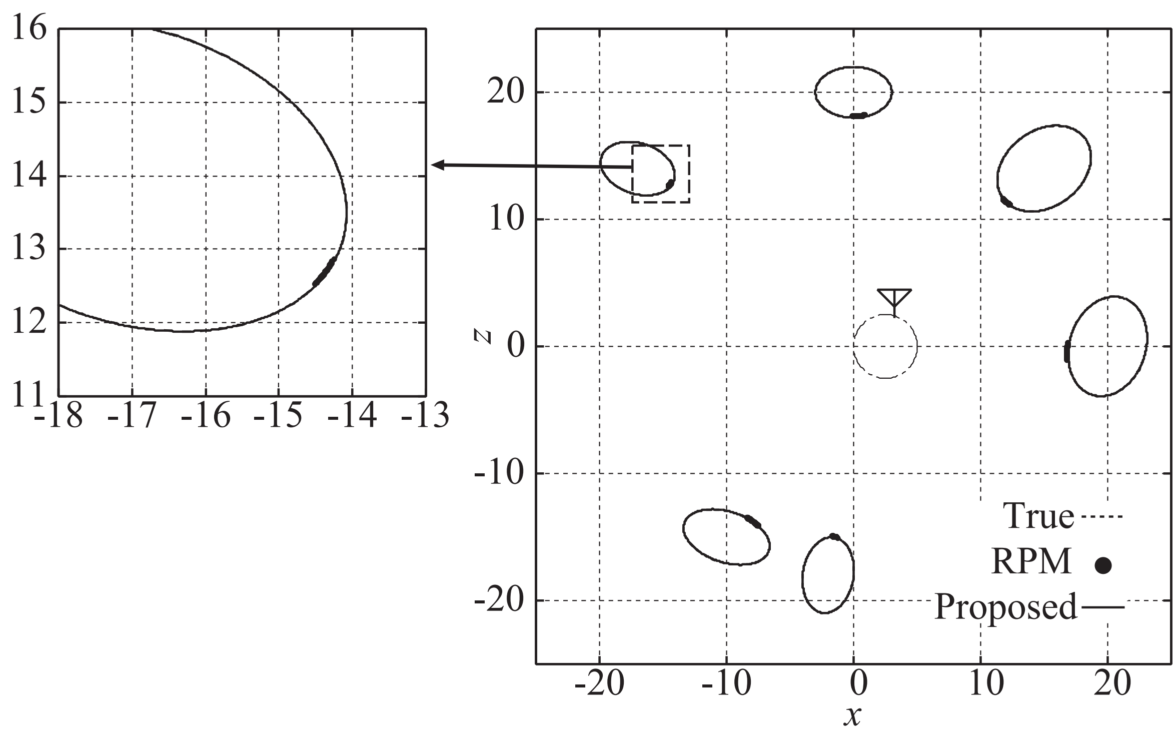

Figure 6: Target points obtained by the RPM and their extrapolation image by the proposed method.

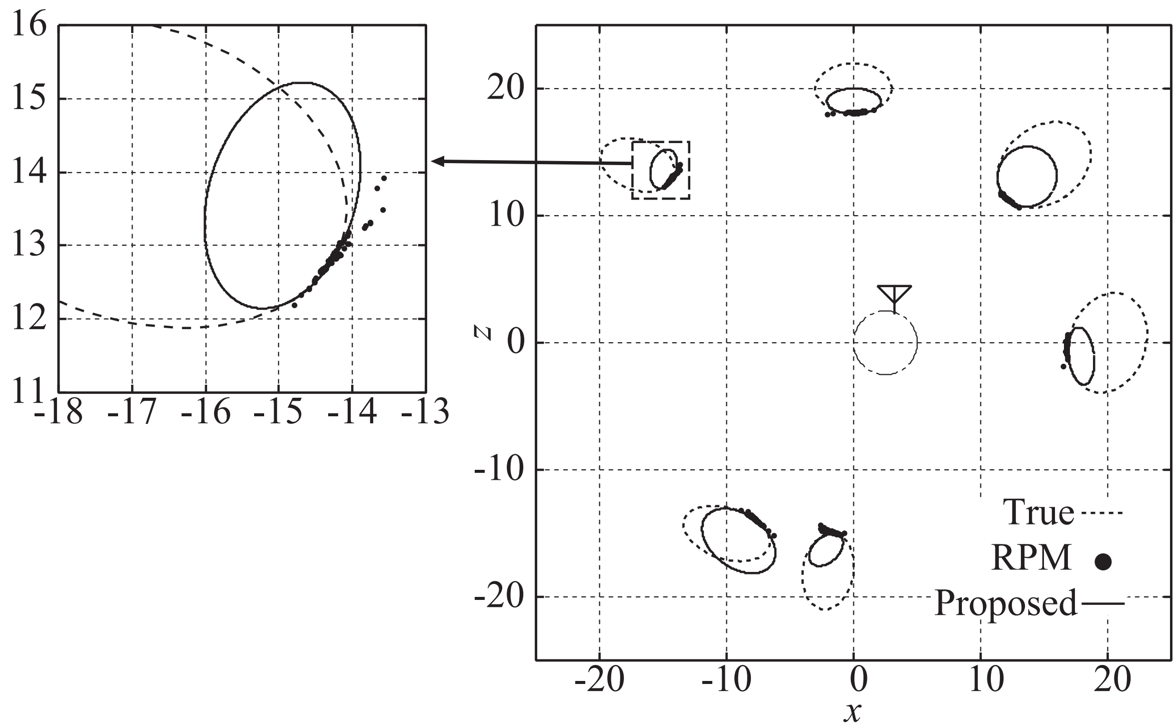

Figure 7: Target points obtained by the RPM and their extrapolation image by the proposed method for S/N = 30 dB.

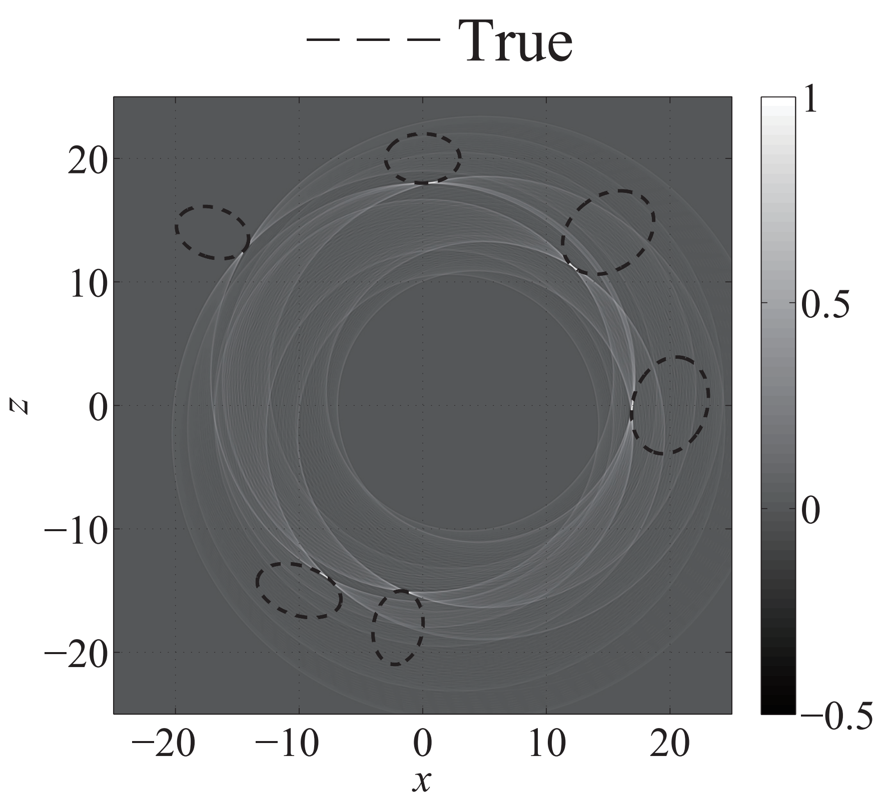

Figure 8: Estimated image with the Synthetic Aperture Radar (SAR).